Supplementary Information

Hydrophobic-Barrier-Assisted Formation of Vertically Layered Capacitive Electrodes within a Single Sheet of Paper

In Hyeok Oh,[a] Sung Min Lee,[a] Yeon Woo Kim,[a] Seyoung Choi,[b] Inho Nam,*[abc] and Suk Tai Chang*[a]

[a] School of Chemical Engineering and Materials Science, Chung-Ang University, 84 Heukseok-ro, Dongjak-gu, Seoul 06974, Republic of Korea

[b] Department of Intelligent Energy and Industry, Chung-Ang-University, 84 Heukseok-ro, Dongjak-gu, Seoul 06974, Republic of Korea

[c] Department of Advanced Materials Engineering, Chung-Ang University, 4726 Seodong-daero, Daedeok-myeon, Anseong-si, Gyeonggi-do 17546, Republic of Korea
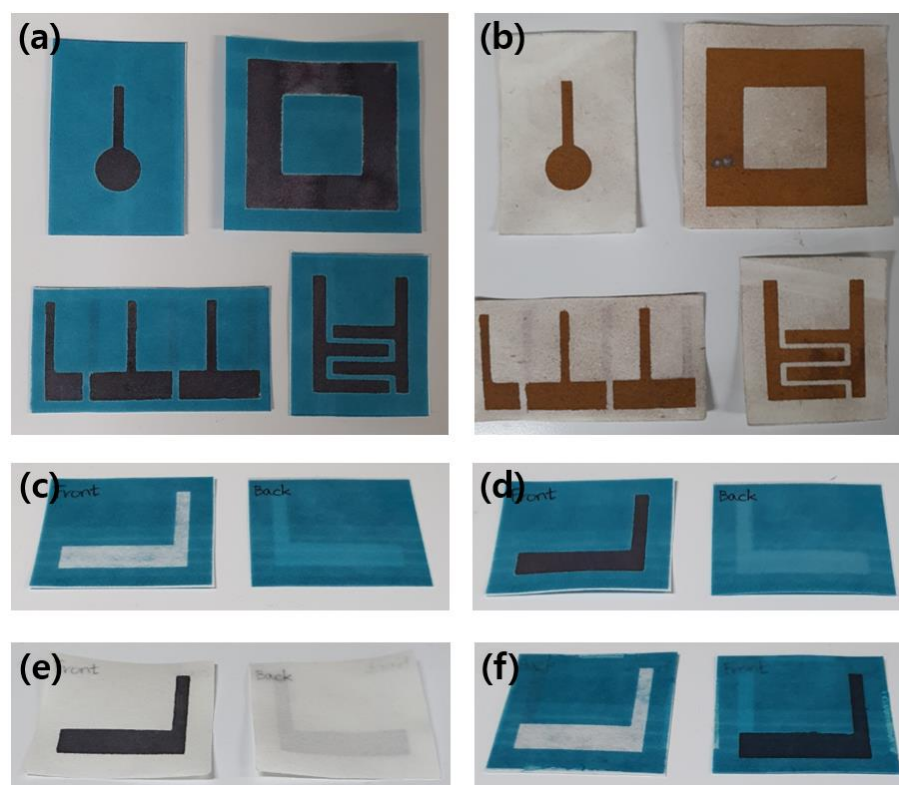

Figure S1. Photographs of various wax-patterned papers. (a) AuNPs deposited in the non-hydrophobic channel spaces. (b) Various patterned Au-paper electrodes. (c) Formation of hydrophobic channels inside the paper. (d) AuNP deposition in a hydrophilic channel within a single sheet of paper. (e) After wax removal. (f) AuNP-paper covered with solid wax.

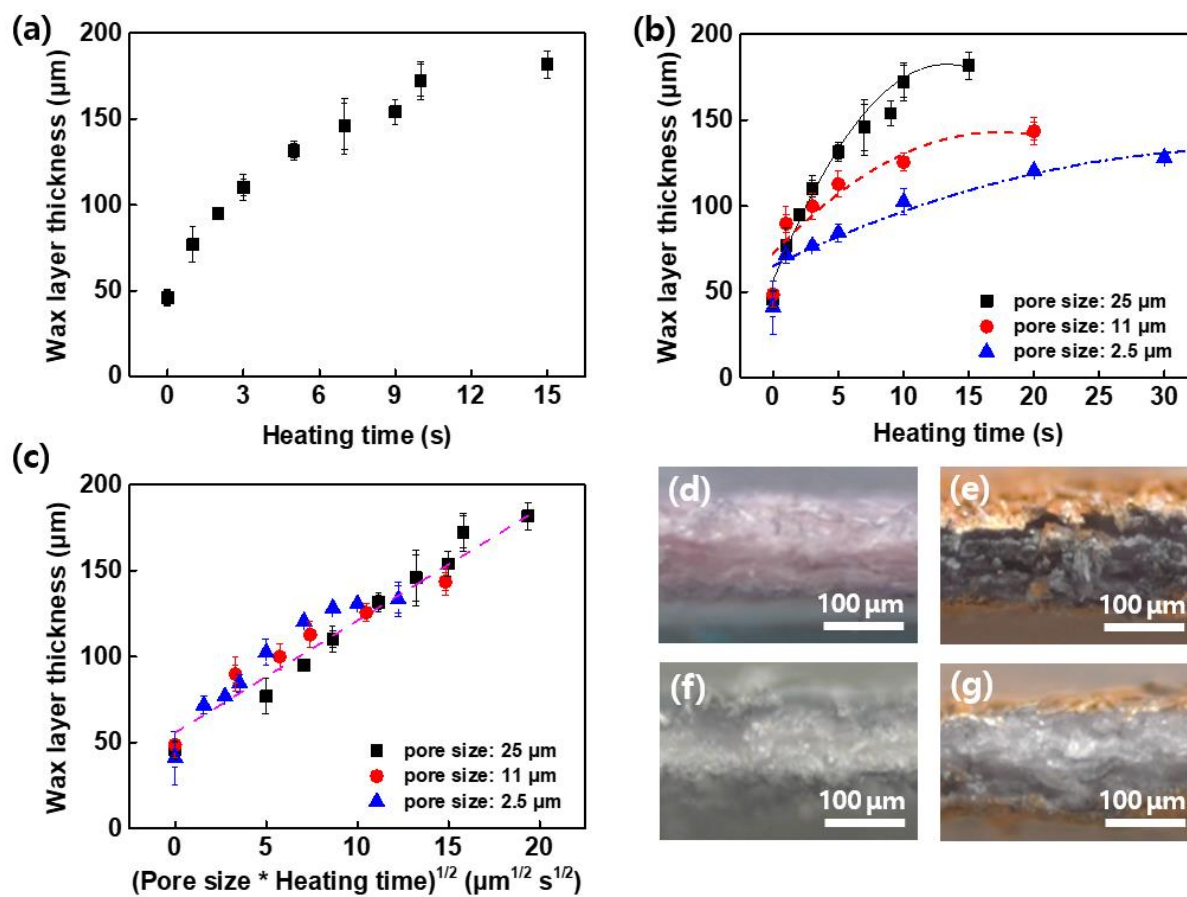* Corresponding author. E-mail : stchang@cau.ac.kr (S. T. Chang), inhonam@cau.ac.kr (I. Nam)

Figure S2. Solid wax characteristics. (a) The thickness of permeated solid wax as a function of heating time. (b) Thickness of permeated wax as a function of heating time for different paper pore sizes. (c) The thickness of permeated wax as a function of the square root of the pore size multiplied by the square root of the heating time. Cross-sectional optical micrographs of AuNPs and the Au-deposited paper (d, e) without wax and (f, g) with wax heated for 3 s.
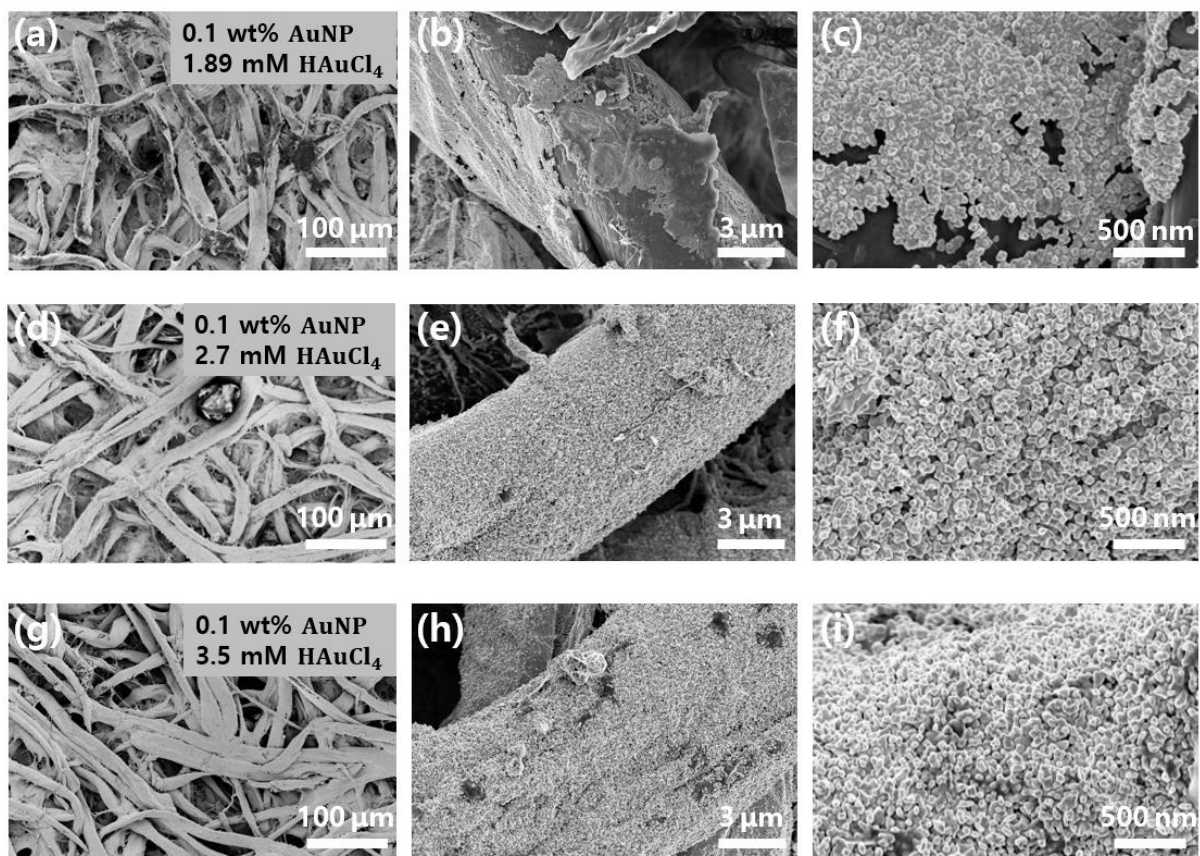
Figure S3. FE-SEM images of the Au-paper electrodes fabricated with 0.1 wt% AuNPs and (a–c) 1.89, (d–f) 2.7, and (g–i) 3.5 mM HAuCl$_4$.
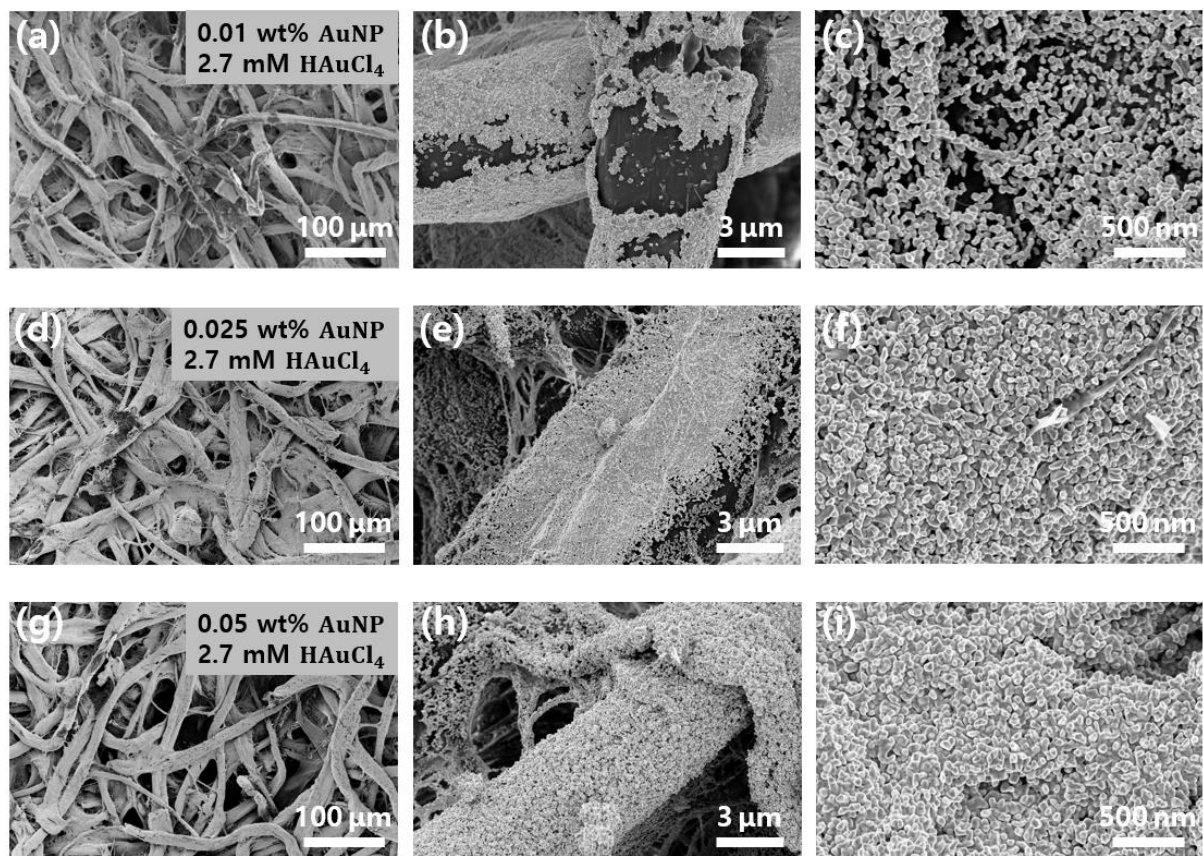
Figure S4. FE-SEM images of the Au-paper electrodes fabricated with 2.7 mM HAuCl$_4$ and (a–c) 0.01, (d–f) 0.025, and (g–i) 0.05 wt% AuNPs.
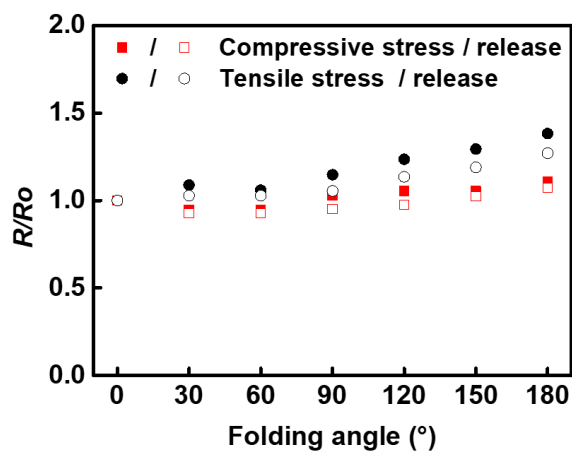
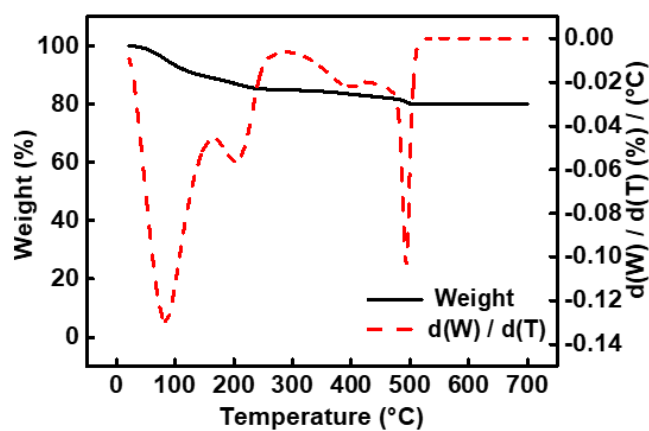**Figure S5.** Resistance profiles from the folding test and resistance recovery on release.
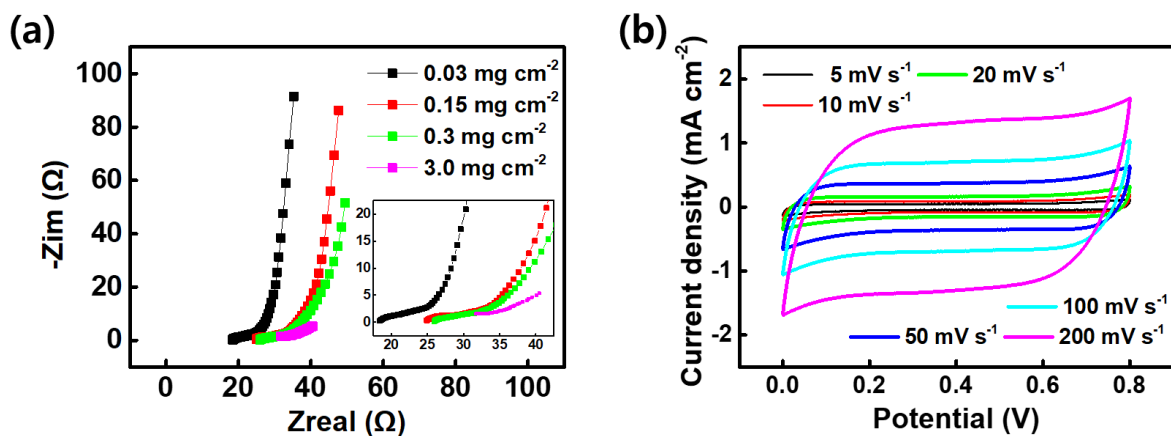

Figure S6. TGA of the MnO_2-Au-paper.

Figure S7. (a) Nyquist plots of the MnO$_2$-Au-paper electrodes with different amounts of MnO$_2$. (b) CVs at different scan rates of the MnO$_2$-Au-paper electrodes with a mass loading of 0.03 mg cm^{-2}.
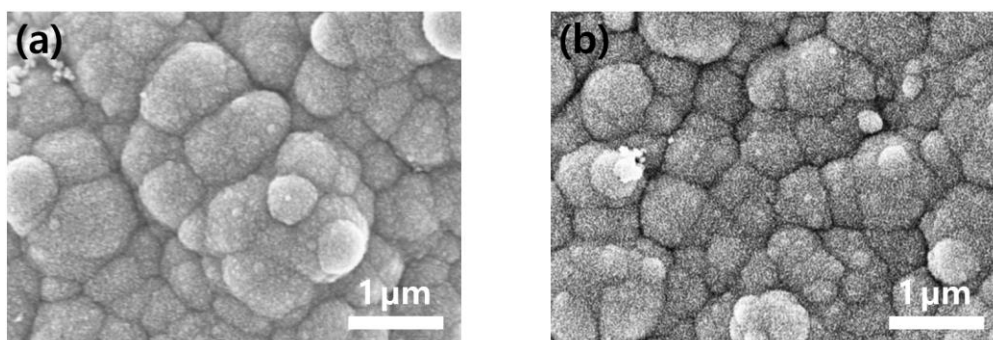

Figure S8. (a) FE-SEM image of the MnO$_2$-Au-paper electrode with the mass loading of 0.3mg cm^{-2}. (b) The electrode after 5000 charge/discharge cycles.
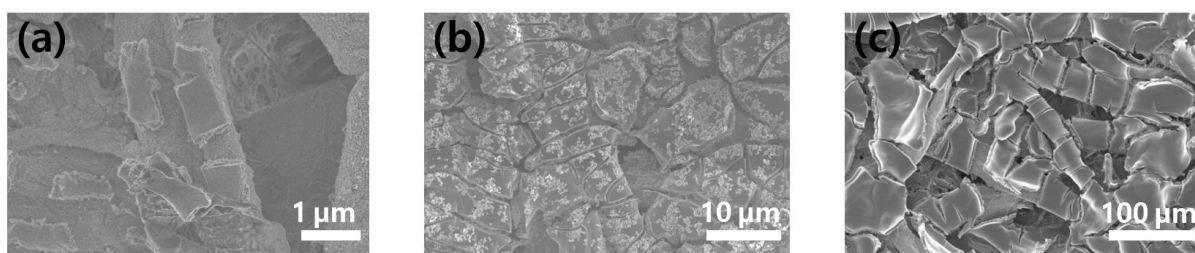

Figure S9. FE-SEM images of the MnO$_2$-Au-paper electrodes witih mass loading of (a) 1.5, (b) 3.0, and (c) 4.0 mg cm^{-2}.
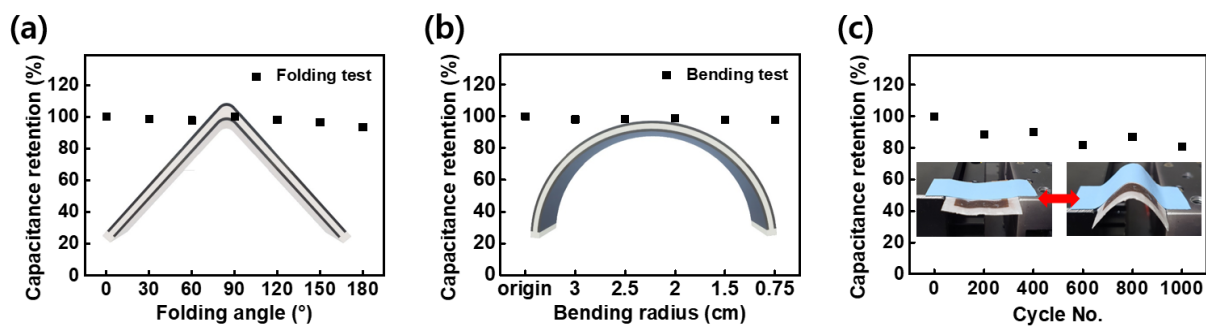
Figure S10. Change in capacitance retention with (a) folding angle and (b) bending radius. (c) Capacitance stability over 1000 cycles with a bending radius of 2.0 cm.
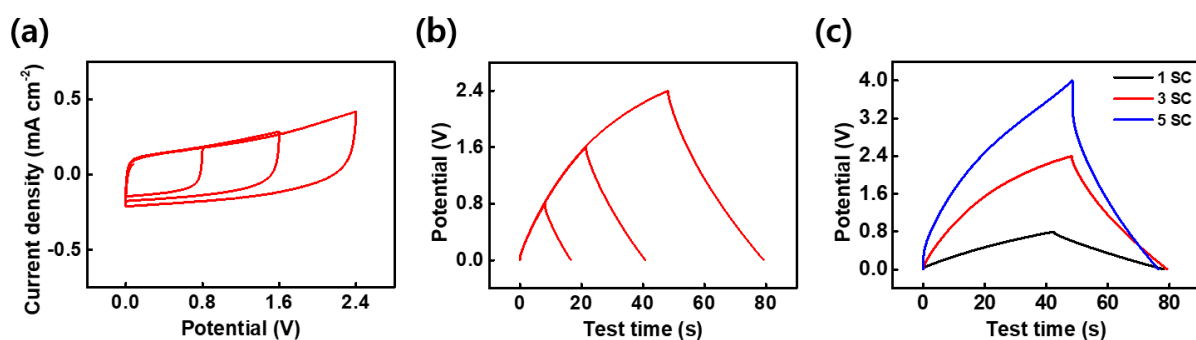

Figure S11. (a) CVs and (b) GCDs of the three-series supercapacitor in different potential ranges. (c) GCD curves at 0.3 mA cm^{-2} of the single, three-series, and five-series supercapacitors.